

# Characterization of a chiral menthyldimethyltin molybdate and its use as an olefin epoxidation catalyst

Marta Abrantes,<sup>a</sup> Anabela A. Valente,<sup>b</sup> Martyn Pillinger,<sup>b</sup> Carlos C. Romão,<sup>a</sup> and Isabel S. Gonçalves,<sup>b,\*</sup>

<sup>a</sup>Instituto de Tecnologia Química e Biológica da Universidade Nova de Lisboa, Av. da Republica, Estação Agronómica Nacional, 2780-157 Oeiras, Portugal

<sup>b</sup>Department of Chemistry, CICECO, University of Aveiro, Campus de Santiago, 3810-193 Aveiro, Portugal

Received 22 November 2006; accepted 12 January 2007

Vibrational spectroscopy and EXAFS studies of an organotin molybdate with the formula  $[(\text{Me})_2(\text{menthyl})\text{Sn}]_2\text{MoO}_4(\text{H}_2\text{O})_{3.5}$  reveal that the compound is polymeric and contains  $[\text{MoO}_4]^{2-}$  tetrahedra coordinated to  $[\text{R}_3\text{Sn}]^+$  cationic spacers. The compound can be used as a recyclable solid catalyst for the selective epoxidation of cyclooctene by *tert*-butylhydroperoxide. In the epoxidation of prochiral olefins such as *trans*- $\beta$ -methylstyrene, the corresponding epoxide isomers are obtained with fairly good to excellent selectivity, albeit with low enantiomeric or diastereomeric excesses.

**KEY WORDS:** molybdenum; tin; (–)-menthyl; organic–inorganic hybrid composites; heterogeneous catalysis; olefin epoxidation.

## 1. Introduction

Research on organic–inorganic hybrid materials with infinite (polymeric) structures has grown exponentially over the last 10 years or so [1–4]. One of the most appealing strategies is the formation of coordination networks through the aggregation via intermolecular bonds of two or more modular units. The self-assembly of organotin cationic fragments such as  $\text{Me}_3\text{Sn}^+$  with different anionic metal-containing species has provided a large family of supramolecular organometallic networks with either 1-dimensional (1D), 2D or 3D architectures [5–23]. In 1993 Fischer and co-workers described a series of compounds with the general formula  $[(\text{R}_3\text{E})_2\text{MO}_4]$  ( $\text{R} = \text{Me}, \text{Et}, n\text{Pr}, n\text{Bu}, \text{or Ph}$ ;  $\text{E} = \text{Sn or Pb}$ ;  $\text{M} = \text{Mo or W}$ ) [19]. The trimethyltin molybdate has a layered structure built up of  $\text{MoO}_4$  tetrahedra and  $\text{Me}_3\text{SnO}_2$  trigonal-bipyramids which are linked by common oxygen atoms. This family was recently extended to include 1D coordination polymers of the type  $(\text{NBu}_4)[(\text{Me}_3\text{Sn})\text{MO}_4]$  ( $\text{M} = \text{Mo}, \text{W}$ ) [21] and the 3D polymer  $(\text{NBu}_4)[(\text{Ph}_3\text{Sn})_3(\text{MoO}_4)_2]$  [20]. Although a large number of potential applications can be envisaged for these hybrid materials [3], particularly in the fields of optics, electronics, gas adsorption and catalysis, most of the published work has been restricted to synthesis and characterization.

We have been studying polymeric organotin molybdates, tungstates and vanadates as catalysts for the liquid-phase oxidation of organic compounds [24–27]. The organotin molybdates  $[(\text{R}_3\text{Sn})_2\text{MoO}_4]$  ( $\text{R} = \text{Me},$

$n\text{Bu}, \text{cyclohexyl}, \text{phenyl}, \text{benzyl}$ ) were tested as catalysts for the oxidation of benzothiophene and for the epoxidation of olefins, using either *tert*-butylhydroperoxide (*t*BuOOH) or aqueous  $\text{H}_2\text{O}_2$  as the oxidant. Under appropriate conditions some of these compounds can be used as recyclable heterogeneous catalysts for the formation of the corresponding epoxides or sulfone in quantitative yield. The catalytic results depend on the nature of the tin-bound R groups and this has led us to explore the possibility of synthesizing chiral catalytic systems by using chiral organotin compounds. Organotin compounds with ligands like the (–)-menthyl group have attracted considerable interest for the preparation of asymmetric heterogeneous catalysts [28, 29]. In the present work, the introduction of chirality into the system  $[(\text{Me}_3\text{Sn})_2\text{MoO}_4]$  has been achieved by the substitution of one of the methyl groups by the (–)-menthyl group. The resultant compound has been characterized in the solid state and examined as a catalyst for the epoxidation of cyclooctene and several unfunctionalized prochiral olefins.

## 2. Experimental

### 2.1. Materials and methods

$\text{Na}_2\text{MoO}_4 \cdot 2\text{H}_2\text{O}$  was obtained from Aldrich and (–)-menthyldimethyltin bromide was synthesized as described in the literature [30]. Microanalyses were performed at the ITQB, Oeiras (by C. Almeida). Thermogravimetric analysis (TGA) was performed using a Mettler TA3000 system at a heating rate of  $5^\circ\text{C min}^{-1}$  under nitrogen. Vibrational spectra were recorded on a

\*To whom correspondence should be addressed.  
E-mail: igoncalves@dq.ua.pt.

Unican Mattson Mod 7000 FTIR spectrometer and on a Bruker RFS 100/S FT Raman spectrometer using a 1064 nm excitation of the Nd/YAG laser.  $^{13}\text{C}$  solid state NMR spectra were recorded at 100.62 MHz on a Bruker Avance 400 (9.4 T) spectrometer.  $^1\text{H}$ - $^{13}\text{C}$  cross-polarization (CP) MAS NMR spectra were acquired with a spinning rate of 7 kHz,  $4.5\ \mu\text{s}$   $^1\text{H}$   $90^\circ$  pulses, a contact time of 2 ms and a recycle delay of 4 s.

X-ray absorption spectra were measured at ca.  $-240^\circ\text{C}$  in transmission mode on beamline BM29 at the ESRF (Grenoble) [31], operating at 6 GeV in 2/3 filling mode with typical currents of 170–200 mA. Each scan was set up to record the pre-edge at 5 eV steps and the post-edge region in  $0.025$ – $0.05\ \text{\AA}^{-1}$  steps, giving a total acquisition time of ca. 45 min. The order-sorting double Si(311) crystal monochromator was detuned by 40% for harmonic rejection. Solid samples were diluted with BN and pressed into 13 mm pellets. The programs EXCALIB and EXBACK (SRS Daresbury Laboratory, UK) were used in the usual manner for calibration and background subtraction of the raw data. EXAFS curve-fitting analyses, by least-squares refinement of the non-Fourier filtered  $k^3$ -weighted EXAFS data, were carried out using the program EXCURVE (version EXCURV98 [32]) using fast curved wave theory [33, 34]. Phase shifts were obtained within this program by *ab-initio* calculations based on the Hedin Lundqvist/von Barth scheme.

## 2.2. Synthesis of $[(\text{Me})_2(\text{menthyl})\text{Sn}]_2\text{MoO}_4(\text{H}_2\text{O})_{3.5}$ (**1**)

A saturated solution of  $\text{Na}_2\text{MoO}_4 \cdot 2\text{H}_2\text{O}$  (0.47 g, 2 mmol) in water (3 ml) was added dropwise to a stirred solution of (–)-menthyldimethyltin bromide (1.45 g, 4 mmol) in acetone (3 ml). A colorless precipitate formed immediately and after 5 min was collected by filtration, washed with water and dried at room temperature *in vacuo*, giving an overall yield of 1.15 g (72%) of **1**. Selected IR (KBr,  $\text{cm}^{-1}$ ): 2954 (m), 2924 (m), 2870 (w), 1456 (w), 1385 (w), 1367 (w), 948 (w), 850 (sh), 835 (vs), 735 (vs), 667 (w), 545 (w). Selected Raman ( $\text{cm}^{-1}$ ): 2926 (vs), 2869 (vs), 2719 (w), 1457 (m), 1194 (m), 1171 (m), 926 (vs), 868 (m), 803 (m), 772 (m), 666 (m), 526 (s), 504 (m), 482 (m), 358 (m), 320 (s), 260 (m).  $^{13}\text{C}$  CP MAS NMR (referenced to  $\text{SiMe}_4$ , see figure 1 for numbering scheme):  $\delta = 45.0$  ( $\text{C}^2$ ), 40.1 ( $\text{C}^{1,6}$ ), 35.5, 32.9 ( $\text{C}^{4,5,8}$ ), 26.6 ( $\text{C}^3$ ), 22.3 ( $\text{C}^{7,9}$ ), 18.1, 16.0 ( $\text{C}^{10}$ ), 3.0 ( $\text{SnMe}_2$ ). Anal. Calcd for  $\text{C}_{24}\text{H}_{57}\text{MoO}_{7.5}\text{Sn}_2$ : C, 36.07; H, 7.19. Found: C, 35.82; H, 6.44.

## 2.3. Catalysis

The liquid-phase catalytic oxidations with 5.5 M *t*BuOOH in decane (10.8 mmol) were carried out at  $55^\circ\text{C}$  under air in a closed batch reactor equipped with a magnetic stirrer and immersed in a thermostated oil bath. The solvent effects were studied under autoge-

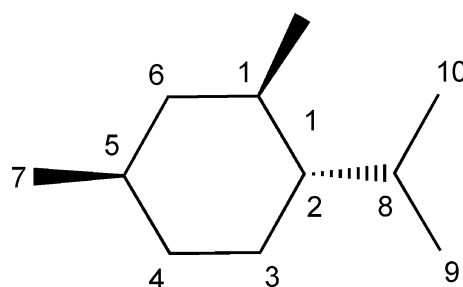


Figure 1 Atom labeling scheme for the assignment of the  $^{13}\text{C}$  CP MAS NMR spectrum of **1**.

neous pressure at  $55^\circ\text{C}$ . A catalyst:substrate:oxidant molar ratio of 1:100:150 was used. Samples were withdrawn periodically and analyzed using a Varian 3800 GC equipped with a capillary column (SPB-5  $20\text{ m} \times 0.25\text{ mm}$  for cyclooctene and CyclosilB  $30\text{ m} \times 0.25\text{ mm}$  for the prochiral olefins) and a flame ionization detector. The products were quantified using calibration curves and *n*-nonane or undecane as internal standard (added after the reaction). The products were identified by GC-MS (HP 5890 Series II GC; HP 5970 Series Mass Selective Detector) using He as carrier gas and by comparing GC retention times with those of fully characterized authentic samples.

## 3. Results and discussion

### 3.1. Synthesis and characterization

The organotin molybdate  $[(\text{Me})_2(\text{menthyl})\text{Sn}]_2\text{MoO}_4(\text{H}_2\text{O})_{3.5}$  (**1**) precipitated upon addition of a saturated aqueous solution of  $\text{Na}_2\text{MoO}_4 \cdot 2\text{H}_2\text{O}$  to a solution of (–)-menthyldimethyltin bromide in acetone. Supporting evidence for the presence of nonremovable  $\text{H}_2\text{O}$  molecules in **1** (at least after prolonged drying *in vacuo* at room temperature) was obtained by carrying out TGA under  $\text{N}_2$ . Upon heating, the weight of compound **1** remains constant from  $25$  to  $100^\circ\text{C}$ . The thermal decomposition of the organic groups takes place in two main steps between  $175$  and  $315^\circ\text{C}$  ( $\text{DTG}_{\text{max}} = 195$  and  $305^\circ\text{C}$ ) and leaves a residual mass of 46%. No further weight changes are observed up to  $700^\circ\text{C}$ . The first step is preceded by a weight loss of 8% which is attributed to dehydration.

Powder X-ray diffraction showed that compound **1** has a low degree of crystallinity and therefore further characterization was carried out using  $^{13}\text{C}$  CP MAS NMR (see experimental section), vibrational spectroscopy and EXAFS. The FTIR spectrum of **1** presents a very strong band at  $835\text{ cm}^{-1}$ , which is assigned to the asymmetric stretch of the  $[\text{MoO}_4]^{2-}$  oxoanion. This mode is observed with medium intensity at  $868\text{ cm}^{-1}$  in the Raman spectrum. The Raman spectrum also contains a strong band at  $926\text{ cm}^{-1}$  for the  $\nu(\text{MoO})$  symmetric stretch, bands at lower wavenumbers (358 and

320  $\text{cm}^{-1}$ ) for the  $\delta(\text{MoO})$  bending modes and a band at 526  $\text{cm}^{-1}$  for the  $\nu(\text{SnC})$  vibration. A weak high frequency shoulder on the latter band is assigned to one of the antisymmetrical (with respect to the  $\text{SnC}_3$  fragment) stretching modes which appears more clearly in the IR spectrum at 546  $\text{cm}^{-1}$ .

The Mo  $K$ -edge EXAFS of **1** was initially fitted by a model comprising 3.9 oxygen atoms at 1.763 Å with a Debye-Waller factor of 0.0034 Å<sup>2</sup>. The close similarity between these values and those previously determined by EXAFS under the same conditions for  $[(\text{Me}_3\text{Sn})_2\text{MoO}_4]$  (4 O at 1.763 Å,  $2\sigma^2 = 0.0028$  Å<sup>2</sup>) strongly points to the presence of a tetrahedral arrangement of four oxygen atoms in the first shell for compound **1**. Both the value of the Mo–O distance and its well-defined nature suggest that each one of these oxygen atoms is bridging rather than terminal, since terminal Mo–O bonds usually have significantly shorter bond lengths of around 1.7 Å. In the crystal structure of the trimethyltin analogue there is only one type of molybdenum atom in the asymmetric unit. The second coordination shell for this atom consists of four tin atoms at the mean distance of 3.84 Å. The Fourier transform of the Mo  $K$ -edge EXAFS of **1** does indicate the presence of shells around 4 Å (figure 2). A statistically significant improvement in the fit was obtained upon addition of a

second shell for one tin atom at 3.80 Å (Table 1), which resulted in a decrease in the goodness-of-fit  $R$ -factor from 23.2 to 21.2%. Although this is consistent with the presence of Mo–O–Sn linkages, the refined coordination number indicates some structural differences compared with the trimethyltin analogue. Caution must however be attached to the accuracy of this coordination number because the refinement of coordination numbers and Debye-Waller factors simultaneously does not always give reliable results, owing to the high correlation of the two parameters. The total number of tin neighbors may be underestimated if there is a high degree of anharmonic static disorder (multiple Mo...Sn interatomic distances). Furthermore, analysis of the low temperature EXAFS of  $[(\text{Me}_3\text{Sn})_2\text{MoO}_4]$  also gave a low coordination number (2) for the tin shell at 3.84 Å [25]. The correct coordination number of four was only obtained after inclusion of a multiple scattering contribution for the Mo–O–Sn unit. This was tried for compound **1** but did not result in any improvement and therefore the final fit shown in Table 1 and figure 2 refers to single scattering calculations only.

The Sn  $K$ -edge EXAFS of **1** was fitted by a three-shell model comprising 4.0 carbon atoms at 2.14 Å, 2.5 oxygen atoms at 2.23 Å and 1 molybdenum atom at 3.79 Å. Addition of the molybdenum shell to the

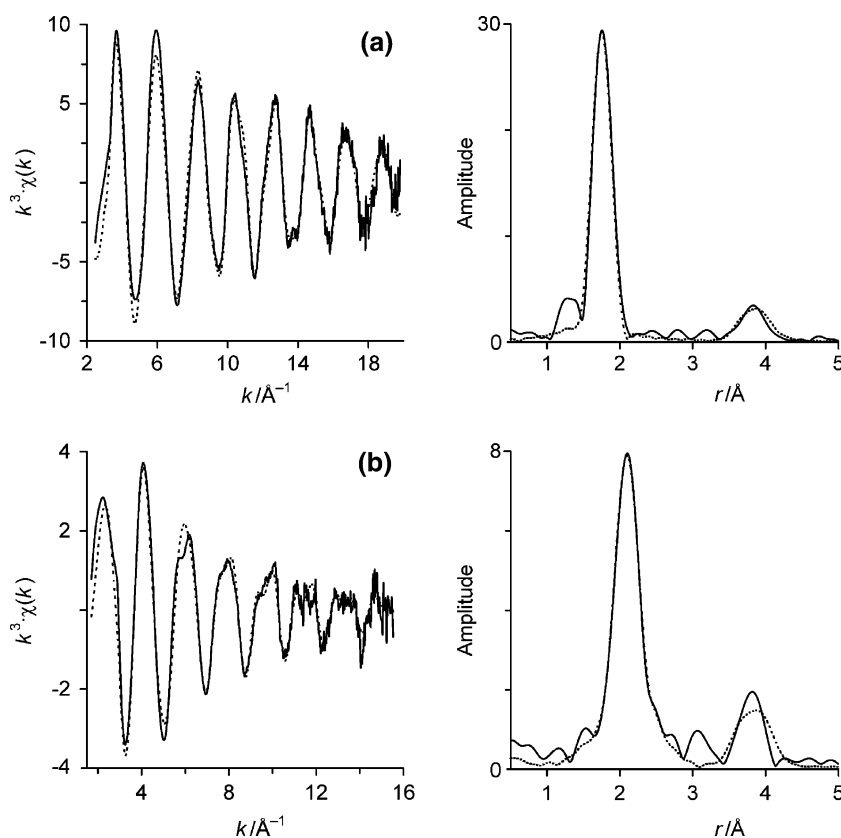


Figure 2 Mo  $K$ -edge (a) and Sn  $K$ -edge (b)  $k^3$ -weighted EXAFS and Fourier transforms of  $[(\text{Me})_2(\text{menthyl})\text{Sn}]_2\text{MoO}_4(\text{H}_2\text{O})_{3.5}$  (**1**). The solid lines represent the experimental data measured at about  $-240$  °C and the dashed lines show fits using the parameters given in Table 1.

Table 1  
Mo *K*-edge and Sn *K*-edge EXAFS-derived structural parameters for  $[(\text{Me})_2(\text{menthyl})\text{Sn}]_2\text{MoO}_4(\text{H}_2\text{O})_{3.5}$  (**1**)<sup>a</sup>

Edge	Atom	CN	$r/\text{\AA}$	$2\sigma^2/\text{\AA}^2$	$E_f/\text{eV}$	$R$ (%)
Mo <i>K</i>	O	3.9(1)	1.763(1)	0.0034(2)	1.4(4)	21.2
	Sn	1.0(3)	3.800(9)	0.0095(14)		
Sn <i>K</i>	C	4.0(3)	2.141(6)	0.0111(10)	-7.2(3)	23.3
	O	2.5(3)	2.228(9)	0.0227(40)		
	Mo	1.0(3)	3.787(7)	0.0135(13)		

<sup>a</sup> CN = Coordination number. Values in parentheses are statistical errors generated in EXCURVE.  $2\sigma^2$  = Debye-Waller factor;  $\sigma$  = root-mean-square internuclear separation.  $E_f$  = edge position (Fermi energy), relative to calculated vacuum zero.

$R = (\int [\Sigma^{\text{theory}} - \Sigma^{\text{exptl}}] k^3 dk / \int [\Sigma^{\text{exptl}}] k^3 dk) \times 100$  %.

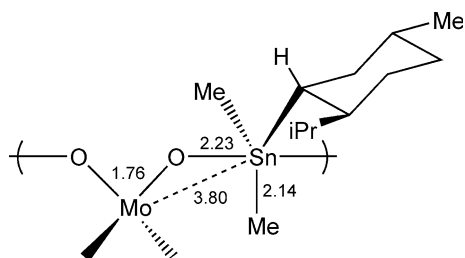


Figure 3 Summary of the EXAFS-derived structural information (distances in Å) for the organotin molybdate **1**.

two-shell model comprising carbon and oxygen reduced the *R*-factor from 29.1 to 23.3%. The Sn–C and Sn–O distances are very similar to those previously determined by EXAFS for the compounds  $[(\text{R}_3\text{Sn})_2\text{MoO}_4]$  (R = Me, *n*Bu) and support the presence of  $\text{R}_3\text{SnO}_2$  units [24, 25]. The Debye-Waller factor for the oxygen shell is quite large and this indicates considerable static disorder in the Sn–O bond. Although the refined coor-

dination number for the third shell is lower than the expected value of two for a connectivity of the type Mo–O–Sn–O–Mo, the Sn...Mo distance is in excellent agreement with that determined from the Mo *K*-edge EXAFS analysis. The EXAFS results therefore support the presence in compound **1** of  $\text{MoO}_4$  tetrahedra and  $\text{Me}_3\text{SnO}_2$  units which are linked by common oxygen atoms (figure 3). As stated above, considerable caution must be attached to the accuracy of the coordination numbers determined for the metal shells at 3.8 Å. Nevertheless, the low values do suggest that the overall connectivity in **1** may be different from that present in the trimethyltin molybdate  $[(\text{Me}_3\text{Sn})_2\text{MoO}_4]$ . One possibility is the insertion of water into some of the Sn–O bonds to give non-linear fragments of the type  $\text{SnO}(\text{H})\text{H}\cdots\text{OMo}$ . This kind of structural motif was reported previously for the 2D coordination polymer  $(\text{Ph}_3\text{Sn})_3\text{Fe}(\text{CN})_6\cdot\text{H}_2\text{O}\cdot 2\text{MeCN}$  [35]. In the crystal structure of this compound one of the CN groups bound to iron is not coordinated to a tin atom. Instead, its N

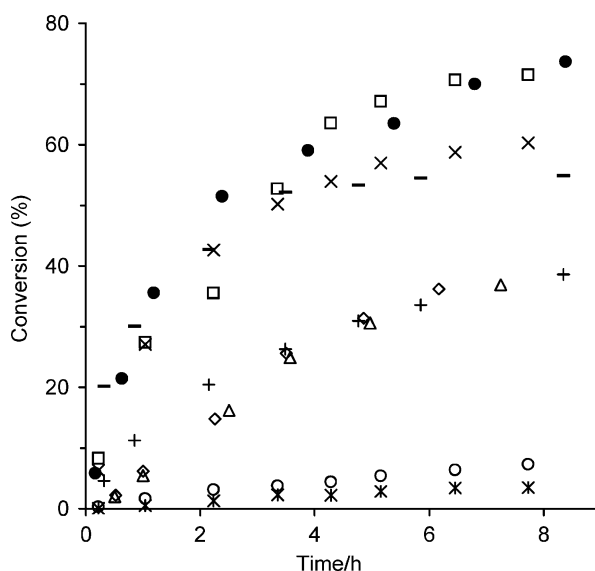
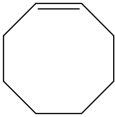

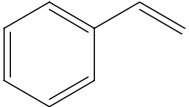
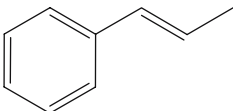
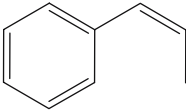
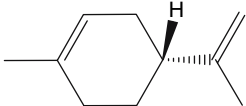
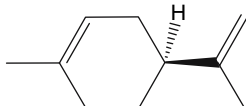


Figure 4 Kinetic profiles of cyclooctene conversion at 55 °C in the presence of **1** without a co-solvent ( $\square$  run 1,  $\diamond$  run 2,  $\Delta$  run 3), with DCM ( $\bullet$ ), MeCN ( $\circ$ ) or EtOH ( $*$ ) using 5.5 M *t*BuOOH in decane, or with DCE using 5.5 M *t*BuOOH in decane ( $\times$ ), 70% aq. *t*BuOOH ( $+$ ) or 30% aq.  $\text{H}_2\text{O}_2$  ( $-$ ) as oxygen donor.

Table 2  
Catalytic results of olefin epoxidation in the presence of **1** using *t*BuOOH as the oxidant in DCM

Substrate	TOF <sup>a</sup> /mol mol <sub>Mo</sub> <sup>-1</sup> h <sup>-1</sup>	Conv. (%) <sup>b</sup>	Select. (%) <sup>b</sup>	Stereoisomer excess (%) <sup>c</sup>
	36	89	100	–
	6	12	100	4 / 1 ee
	2	25	94	0 / 0 ee
	18	68	100	0 / 0 ee
	18	73	100	7 / 2 ee
 (R)-(+)-limonene	39	85	89	5 / 5 de
 (S)-(-)-limonene	49	97	68	7 / 5 de
DL-limonene	41	90	79	

<sup>a</sup> Turnover frequency calculated at 1 h reaction. <sup>b</sup> Olefin conversion and total epoxides selectivity calculated at 24 h. <sup>c</sup> Enantiomeric (ee) or diastereomeric (de) excesses calculated at 1 h / 24 h.

atom is hydrogen bonded to a water molecule that is coordinated to a tin atom. The authors suggested that the coordination of all six N atoms in a Fe(CN)<sub>6</sub> unit to a tin atom was not possible because of steric interference between the bulky Ph<sub>3</sub>Sn<sup>+</sup> groups.

### 3.2. Catalytic olefin epoxidation

Catalytic tests were first carried out using *cis*-cyclooctene as a model substrate and *t*BuOOH (5.5 M in decane) as oxygen donor, at 55 °C. A biphasic solid-liquid system is obtained by the addition of **1** to the reaction solution containing the olefin and the oxidant. Control experiments without catalyst or in the presence of (–)-menthyltrimethyltin bromide showed negligible cyclooctene conversion during 5 h reaction. In the presence of **1**, the oxidation of cyclooctene without a co-solvent yields 1,2-epoxycyclooctane as the only product up to at least 80% conversion. These results indicate

that the active species contain molybdenum. The excellent product selectivity was also observed for the other organotin molybdates that we have studied to date [24, 26]. The initial catalytic activity of 50 mol mol<sub>Mo</sub><sup>-1</sup>h<sup>-1</sup> for **1** is higher than the previous best of 21 mol mol<sub>Mo</sub><sup>-1</sup>h<sup>-1</sup> for [(*n*Bu<sub>3</sub>Sn)<sub>2</sub>MoO<sub>4</sub>]. After 7 h reaction, cyclooctene conversion is about 70% for both catalysts.

The solvent effect on cyclooctene epoxidation in the presence of **1** was investigated, using dichloromethane (DCM), 1,2-dichloroethane (DCE), acetonitrile (MeCN) or ethanol (EtOH) as co-solvent. For all solvents the corresponding epoxide was the only observed product throughout 24 h reaction. Whereas the addition of DCM or DCE has no major effect on the reaction rate, the addition of MeCN or EtOH is detrimental (figure 4). It has been proposed for *t*BuOOH-based epoxidations of olefins with Mo<sup>VI</sup> complexes that the active oxidizing species are formed via the coordination of the oxidant to the metal centre, thereby increasing the oxidizing power



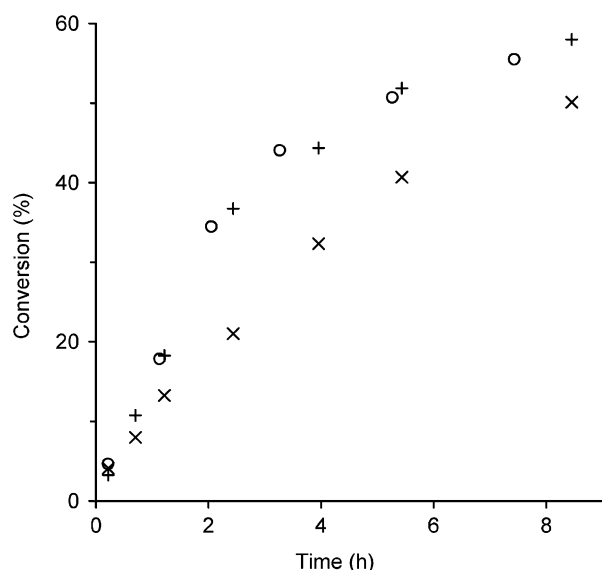


Figure 5 Kinetic profiles of the epoxidation of *cis*- $\beta$ -methylstyrene in DCM (○) and *trans*- $\beta$ -methylstyrene in DCM (+) or without co-solvent (×) in the presence of **1**, using 5.5 M *t*BuOOH in decane at 55 °C.

of the peroxo group of *t*BuOOH. Assuming that a similar elementary step occurs for **1**, coordinating solvent molecules such as MeCN and EtOH may retard or inhibit the epoxidation reaction by acting as competitive ligands to *t*BuOOH for coordination to the metal centre.

The use of aqueous *t*BuOOH instead of anhydrous *t*BuOOH decreases the overall reaction rate (figure 4). When 30% aq.  $H_2O_2$  was used instead of 70% aq. *t*BuOOH the initial activity increased from 15 to 64 mol mol<sup>-1</sup><sub>Mo</sub> h<sup>-1</sup>, but after 3 h the reaction practically stopped. A second charge of  $H_2O_2$  (same amount as the first charge) after 24 h resulted in only 6% conversion at 96 h, suggesting that water severely deactivates the catalyst.

The catalytic stability of **1** was checked by recycling the solid recovered by centrifugation, washing with *n*-hexane and drying at room temperature. The reaction rate decreased from the first to the second run and then remained roughly constant (figure 4), leading to ca. 70% conversion at 24 h. The decrease in catalytic activity could be caused by the coordination of *tert*-butanol (produced in the consumption of *t*BuOOH during the first reaction cycle) to the active metal centers [36].

The catalytic performance of **1** was further explored for the epoxidation of the prochiral olefins *cis*- and *trans*- $\beta$ -methylstyrene (*cis*-MeSty and *trans*-MeSty), 1-octene and styrene, and of racemic DL-limonene, as well as of the isolated isomers (R)- and (S)-limonene, using 5.5 M *t*BuOOH in decane and DCM as co-solvent. For all substrates, compound **1** yielded the corresponding epoxide isomers with fairly good to excellent selectivity, albeit with rather low or negligible enantiomeric or diastereomeric (ee or de) excesses (Table 2).

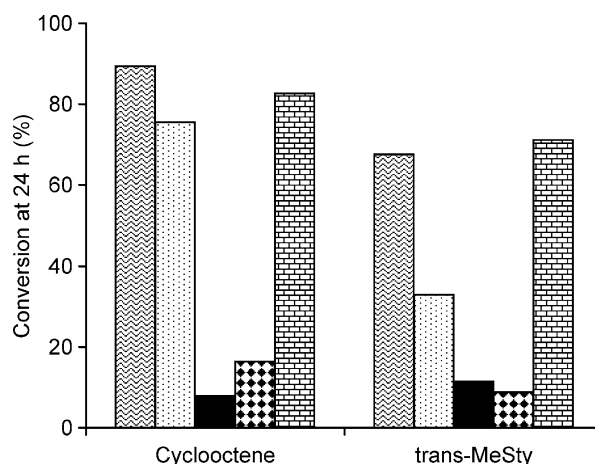


Figure 6 Conversion of cyclooctene and *trans*- $\beta$ -methylstyrene at 55 °C using 5.5 M *t*BuOOH in decane without a co-solvent (bricks) or in the presence of DCM (waves), DCE (dots), EtOH (black) or MeCN (diamonds).

For *cis*-MeSty and *trans*-MeSty the kinetic profiles are practically coincident and excellent product selectivity (100%) was observed in terms of total epoxide products formed (figure 5, Table 2). The reaction products were the enantiomers of 1-phenylpropylene oxide: The (S,R)-(-) and (R,S)-(-) enantiomers were produced from *cis*-MeSty, while the (R,R)-(+) and (S,S)-(-) enantiomers were produced from *trans*-MeSty. For *cis*-MeSty the ee dropped from 15% at 5% conversion to 2% at 73% conversion (24 h). For *trans*-MeSty, the ee was 3% (1*R*,2*R*) at the beginning of the reaction (4% conversion) and negligible above 10% conversion.

The reactions of styrene and 1-octene in the presence of **1** were much slower than those of the more substituted olefins (Table 2). Based on the mechanistic assumptions mentioned above one would expect a lower reactivity for the less substituted olefins, since the higher electronic density of an internal olefinic double bond (compared with a terminal C=C bond) should favor nucleophilic attack on an electrophilic oxidizing species. Styrene epoxidation gave a racemic mixture of (R)- and (S)-styrene oxide up to 25% conversion at 24 h. For 1-octene, (R)-(+)- and (S)-(-)-1,2-epoxyoctane were the only products, formed with an ee of 4% (R) at 6% conversion decreasing to 1% at 12% conversion.

Although limonene possesses an exo- and endocyclic double bond, in the presence of **1** the epoxidation of the cyclo double bond appears to be the most favored and reveals fairly good regioselectivity. When (R)-(+)-, (S)-(-)-limonene or DL-limonene are the substrates, the total amount of 1,2-epoxide isomers yielded at 85–97% conversion is 65–67% (24 h, Table 2): (1*R*,4*R*)-(+)-*cis*- and (1*S*,4*R*)-(+)-*trans*-limonene-1,2-epoxide are produced from (R)-(+)-limonene, (1*S*,4*S*)-(-)-*cis*- and (1*R*,4*S*)-(-)-*trans*-limonene-1,2-epoxide are produced from (S)-(-)-limonene, and in

the reaction of DL-limonene all four isomers are produced. Limonene diepoxides (1,2:8,9-diepoxy-) are formed and epoxide ring opening of limonene oxide into the corresponding diol is also observed. For (R)-(+)- or (S)-(-)-limonene, a de of 5–7% is obtained up to 85–97% conversion (Table 2). A somewhat favorable attack on the pro-*cis* face of the endo-cyclic double bond to the corresponding isomer is observed, probably because it is the least hindered. Similar results were obtained for the DL-limonene racemic mixture, which gave the four limonene-1,2-epoxide isomers (67% yield at 90% conversion).

With *trans*- $\beta$ -methylstyrene as the substrate, the solvent effect on catalytic activity follows a similar trend to that observed with cyclooctene and conversions at 24 h decreased in the following order (figure 6): no co-solvent  $\equiv$  DCM > DCE > MeCN  $\equiv$  EtOH. No significant influence of the solvent on enantioselectivity was observed.

#### 4. Concluding remarks

This work describes our first attempt to prepare a chiral organotin molybdate polymer for asymmetric olefin epoxidation catalysis. In terms of activity and total epoxide selectivity, the material is at least as good as or even outperforms previously studied triorganotin molybdates such as  $[(n\text{Bu}_3\text{Sn})_2\text{MoO}_4]$ . In the epoxidation of prochiral olefins, the observed enantiomeric or diastereomeric excesses were very low, which may be partly due to the fact that the chiral ligand is far from the  $\text{Mo}^{\text{VI}}$  centre responsible for the catalytic epoxidation. Changing the nature of the ligand or using  $[\text{R}_3\text{Sn}]^+$  cations with three chiral groups may lead to better results and these studies are currently underway in our laboratories.

#### Acknowledgments

The authors are grateful to the FCT, OE and FEDER for funding (Project POCI/CTM/58507/2004). We acknowledge the European Synchrotron Radiation Facility for provision of synchrotron radiation facilities and we would like to thank Silvia Ramos for assistance in using beamline BM29.

#### References

- [1] P.J. Hargman, D. Hargman and J. Zubieta, *Angew. Chem. Int. Ed.* 38 (1999) 2638.
- [2] B. Moulton and M.J. Zaworotko, *Chem. Rev.* 101 (2001) 1629.
- [3] C. Janiak, *Dalton Trans.* (2003) 2781.
- [4] M. Oh, G.B. Carpenter and D.A. Sweigart, *Acc. Chem. Res.* 37 (2004) 1.
- [5] J. Lu, W.T.A. Harrison and A.J. Jacobson, *Angew. Chem. Int. Ed. Engl.* 34 (1995) 2557.
- [6] T. Niu, J. Lu, X. Wang, J.D. Korp and A.J. Jacobson, *Inorg. Chem.* 37 (1998) 5324.
- [7] T. Niu and A.J. Jacobson, *Inorg. Chem.* 38 (1999) 5346.
- [8] P. Brandt, A.K. Brimah and R.D. Fischer, *Angew. Chem. Int. Ed. Engl.* 27 (1988) 1521.
- [9] U. Behrens, A.K. Brimah and R.D. Fischer, *J. Organomet. Chem.* 411 (1991) 325.
- [10] U. Behrens, A.K. Brimah, T.M. Soliman, R.D. Fischer, D.C. Apperley, N.A. Davies and R.K. Harris, *Organometallics* 11 (1992) 1718.
- [11] P. Schwarz, S. Eller, E. Siebel, T.M. Soliman, R.D. Fischer, D.C. Apperley, N.A. Davies and R.K. Harris, *Angew. Chem. Int. Ed. Engl.* 35 (1996) 1525.
- [12] E. Sieber and R.D. Fischer, *Chem. Eur. J.* 3 (1997) 1987.
- [13] P. Schwarz, E. Siebel, R.D. Fischer, N.A. Davies, D.C. Apperley and R.K. Harris, *Chem. Eur. J.* 4 (1998) 919.
- [14] E.-M. Poll, J.-U. Schütze, R.D. Fischer, N.A. Davies, D.C. Apperley and R.K. Harris, *J. Organomet. Chem.* 621 (2001) 254.
- [15] R. Eckhardt, H. Hanika-Heidl and R.D. Fischer, *Chem. Eur. J.* 9 (2003) 1795.
- [16] H. Hanika-Heidl and R.D. Fischer, *Microporous Mesoporous Mater.* 73 (2004) 65.
- [17] E. Herdtweck, P. Kiprof, W.A. Herrmann, J.G. Kuchler and I. Degnan, *Z. Naturforsch.* 45b (1990) 937.
- [18] B. Kanellakopulos, K. Raptis, B. Nuber and M.L. Ziegler, *Z. Naturforsch.* 46b (1991) 15.
- [19] U. Behrens, A.K. Brimah, K. Yünlü and R.D. Fischer, *Angew. Chem. Int. Ed. Engl.* 32 (1993) 82.
- [20] F. Rosenlund, M. Kondracka and K. Merzweiler, *Z. Anorg. Allg. Chem.* 629 (2003) 2573.
- [21] F. Rosenlund, M. Kondracka and K. Merzweiler, *Z. Anorg. Allg. Chem.* 631 (2005) 2919.
- [22] E.-M. Poll, M. Rehbein, M. Eppe and R.D. Fischer, *Supramol. Chem.* 15 (2003) 409.
- [23] F. Rosenlund and K. Merzweiler, *Z. Anorg. Allg. Chem.* 627 (2001) 2403.
- [24] M. Abrantes, A.A. Valente, M. Pillinger, I.S. Gonçalves, J. Rocha and C.C. Romão, *J. Catal.* 209 (2002) 237.
- [25] M. Abrantes, A.A. Valente, M. Pillinger, I.S. Gonçalves, J. Rocha and C.C. Romão, *Chem. Eur. J.* 9 (2003) 2685.
- [26] M. Abrantes, A.A. Valente, I.S. Gonçalves, M. Pillinger and C.C. Romão, *J. Mol. Catal. A: Chem.* 238 (2005) 51.
- [27] M. Abrantes, M.S. Balula, A.A. Valente, F.A.A. Paz, M. Pillinger, C.C. Romão, J. Rocha and I.S. Gonçalves, *J. Inorg. Organomet. Polym. Mater.* (in press).
- [28] A. de Mallmann, O. Lot, N. Perrier, F. Lefebvre, C.C. Santini and J.M. Basset, *Organometallics* 17 (1998) 1031.
- [29] M.B. Faraoni, A.D. Ayala, V. Vetere, M.L. Casella, O.A. Ferretti and J.C. Podestá, *Appl. Organomet. Chem.* 19 (2005) 465.
- [30] H. Schumann, B.C. Wassermann and F.E. Hahn, *Organometallics* 11 (1992) 2803.
- [31] A. Filipponi, M. Borowski, D.T. Bowron, S. Ansell, A.D. Cicco, S.D. Panfilis and J.-P. Itié, *Rev. Sci. Instrum.* 71 (2000) 2422.
- [32] N. Binsted, EXCURV98, CCLRC Daresbury Laboratory computer programme, 1998.
- [33] S.J. Gurman, N. Binsted and I. Ross, *J. Phys. C* 17 (1984) 143.
- [34] S.J. Gurman, N. Binsted and I. Ross, *J. Phys. C* 19 (1986) 1845.
- [35] J. Lu, W.T.A. Harrison and A.J. Jacobson, *Inorg. Chem.* 35 (1996) 4271.
- [36] A. Al-Ajlouni, A.A. Valente, C.D. Nunes, M. Pillinger, A.M. Santos, J. Zhao, C.C. Romão, I.S. Gonçalves and F.E. Kühn, *Eur. J. Inorg. Chem.* (2005) 1716.